 ©2004 Kvantovaya Elektronika and Turpion Ltd

PACS numbers: 85.70.Sq; 42.55.-f
DOI: 10.1070/QE2004v034n10ABEH002693

Use of thin discs in Faraday isolators for high-average-power lasers

I.B. Mukhin, E.A. Khazanov

***Abstract*. The possibility of development of a Faraday isolator consisting of several thin magnetooptical discs was investigated. An analytical and numerical analysis was performed taking into account the photoelastic effect, the temperature dependence of the Verdet constant, and the Fresnel reflections between the discs. The depolarisation ratio caused by thermal effects was shown to be much weaker in the disc geometry than in the rod geometry. The results obtained suggest that it is possible to make a Faraday isolator for laser radiation with a multikilowatt average output power.**

Keywords: *Faraday isolator, photoelastic effect, depolarisation.*

1. Introduction

The investigation of thermal effects related to laser radiation absorption in different optical elements is made topical by the growth of output power of cw and repetitively pulsed lasers. A Faraday isolator undergoes a strong thermal self-action, because the absorption in magnetoactive media is strong. The transversely nonuniform temperature distribution is responsible for wavefront distortion (a thermal lens) owing to the temperature dependence of the refractive index, for the nonuniform distribution of the angle of polarisation plane rotation arising from the temperature dependence of the Verdet constant, and for the linear birefringence caused by thermoelastic stress (the photoelastic effect). The last two effects lead to polarisation distortions and hence to impairment of isolation.

For rod-shaped magnetoactive elements, these effects were comprehensively investigated in Refs [1 – 11] (see also references therein). In these works it was shown that the photoelastic effect makes the greatest contribution to the depolarisation ratio, while the temperature dependence of the Verdet constant can be neglected. New schemes of Faraday isolators were proposed and investigated in Ref. [1] in order to increase the average power of transmitted radiation. Instead of one Faraday element which rotates the plane of polarisation by 45°, these schemes make use of two 22.5-degree Faraday elements and a reciprocal optical element between them. In this case, the distortions arising in the pass through the first element are partially compensated for in the pass through the second one.

Summarising the results outlined in the above literature, one may draw the following conclusion: with the use of rod-shaped elements it is possible to make reliable isolators for the radiation with an average power up to 1 kW. Advancement to the multikilowatt range calls for new approaches related to the change of geometry of the active elements of Faraday elements. Employing slabs is highly efficient [12], but only for rectangular (elliptical) beams.

Our work is concerned with the investigation of a Faraday isolator which is made up of a set of thin discs cooled through the optical surface. This geometry leads to a reduction of the transverse temperature gradient in the discs and hence to a decrease of the linear birefringence.

2. Depolarisation ratio in discoid Faraday isolators

In the absence of thermal effects, all isolators depicted in Fig. 1 offer total radiation transmission in the first pass (from left to right) and reject radiation in the second one. The overall disc thickness L should be the same as in the cylindrical geometry, because the total rotation angle of the plane of polarisation in the radiation pass though all the discs should be equal to 45°. Hence, use should be made of N discs of thickness $h = L/N$ each. The occurrence of thermal effects leads to the emergence of a field transmitted through polariser (*1*) in the second pass. The local depolarisation ratio of a Faraday isolator is defined as

$$\Gamma(r,\varphi) = \frac{|\boldsymbol{E}_x(r,\varphi)|^2}{|\boldsymbol{E}(r,\varphi)|^2}, \tag{1}$$

where $\boldsymbol{E}$ is the complex amplitude of the field incident on polariser (*1*) in the backward pass; $\boldsymbol{E}_x$ is the complex amplitude of the field transmitted through polariser (*1*); r and φ are the polar coordinates. Of greatest interest is the depolarisation ratio integrated over the beam cross section:

$$\gamma = \frac{\int_0^{2\pi} \mathrm{d}\varphi \int_0^R \Gamma I(r) r \mathrm{d}r}{\int_0^{2\pi} \mathrm{d}\varphi \int_0^R I(r) r \mathrm{d}r}. \tag{2}$$

Here, $I(r)$ is the laser beam intensity and R is the radius of the discs. In what follows we assume that the laser beam of

I.B. Mukhin, E.A. Khazanov Institute of Applied Physics, Russian Academy of Sciences, ul. Ul'yanova 46, 603950 Nizhnii Novgorod, Russia

Received 13 April 2004; revision received 30 June 2004
Kvantovaya Elektronika **34** (10) 973 – 978 (2004)
Translated by E.N. Ragozin

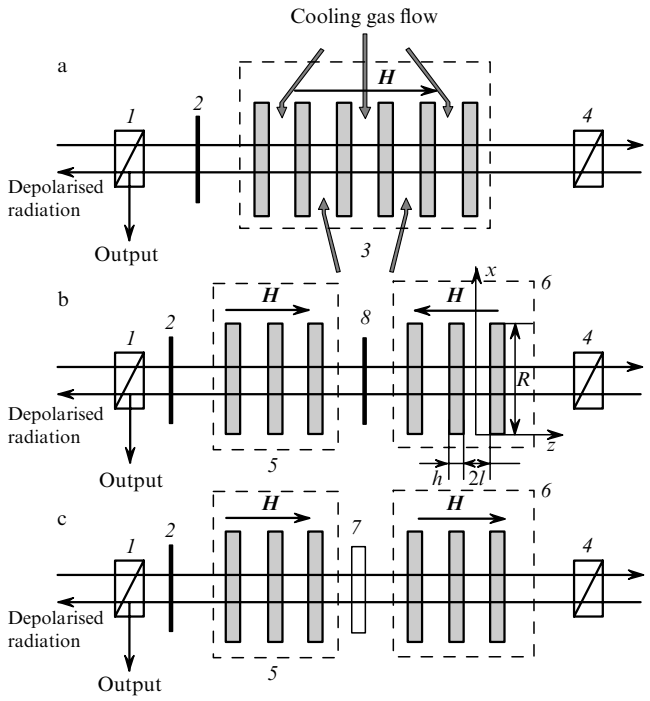

Figure 1. Conventional Faraday isolator scheme (a) and schemes with compensation for polarisation distortions (b, c) [2]: (*1*, *4*) polarisers; (*2*, *8*) $\lambda/2$ plates; (*3*) 45-degree Faraday rotator; (*5*) 22.5-degree clockwise Faraday rotator; (*6*) 22.5-degree counterclockwise Faraday rotator; (*7*) reciprocal polarisation rotator.

radius r_0 possesses a super-Gaussian shape with an exponent m:

$$I(r) = I_0 \exp\left(-\frac{r^{2m}}{r_0^{2m}}\right). \tag{3}$$

For a linear birefringence phase difference δ_{lin} far smaller than unity, Khazanov [1] obtained the expressions for $\Gamma_{0,\text{L,R}}$:

$$\Gamma_0 = \frac{2}{\pi^2}\delta_{\text{lin}}^2 \sin^2\left(2\Psi - \frac{\pi}{4}\right) + O(\delta_{\text{lin}}^4), \tag{4}$$

$$\Gamma_{\text{L}} = \frac{16\delta_{\text{lin}}^4}{\pi^4}\left[a + b\left(\frac{\sin 4\Psi}{\sqrt{2}} - \frac{\cos 4\Psi}{\sqrt{2}}\right)\right]^2 + O(\delta_{\text{lin}}^6), \tag{5}$$

$$\Gamma_{\text{R}} = \frac{16\delta_{\text{lin}}^4}{\pi^4}a^2 + O(\delta_{\text{lin}}^6), \tag{6}$$

where $a = (\pi - 2\sqrt{2})/8$; $b = (2 - \sqrt{2})/4$; Ψ is the angle of eigenpolarisation inclination; and the indices 0, L, and R refer to the schemes in Figs 1a, 1b, and 1c, respectively. For a magnetoactive crystal with the orientations [001] and [111], the angle Ψ is defined by the formulas [10]

$$\tan(2\Psi - 2\theta) = \xi \tan(2\varphi - 2\theta) \text{ for the [001] orientation,} \tag{7}$$

$$\Psi = \varphi \qquad \text{for the [111] orientation,} \tag{8}$$

where θ is the angle between the crystallographic axis and the x axis; $\xi = (p_{11} - p_{12})/(2p_{44})$; and p_{ij} are the photoelasticity coefficients. Therefore, to determine Γ and, consequently, γ requires calculating δ_{lin}. This quantity depends strongly on the geometry: on the disc dimensions R and h and the laser beam radius r_0. We determine the integral depolarisation ratio for three cases between the disc dimensions and the laser beam radius: $h \ll r_0 \ll R$ (a thin wide-aperture disc), $h \ll r_0$, $r_0 \simeq R$ (a thin disc), and R, $r_0 \simeq h$ (the general case).

Thin wide-aperture disc ($h \ll r_0 \ll R$). Under this approximation, the disc may be considered to be so thin that all heat is removed across its faces and does not propagate in the radial direction. The disc is in a planar stressed state [13], and its radius is greater than the laser beam radius to an extent than integration in expression (2) can be extended to infinity.

In the case of a planar stressed state, N discs will give rise to a linear birefringence phase difference [14]

$$\delta_{\text{lin}} = 4\pi\frac{L}{\lambda}q(\varphi)Q_{\text{disc}}\frac{1}{r^2}\int_0^r r^2\left[\frac{\mathrm{d}\tilde{T}(r)}{\mathrm{d}r}\right]\mathrm{d}r, \tag{9}$$

where

$$q(\varphi) = \begin{cases} \left[\dfrac{1 + \xi^2\tan^2(2\varphi - 2\theta)}{1 + \tan^2(2\varphi - 2\theta)}\right]^{1/2} & \text{for the [001] orientation,} \\ \dfrac{1 + 2\xi}{3} & \text{for the [111] orientation;} \end{cases} \tag{10}$$

$$Q_{\text{disc}} = \left(\frac{1}{L}\frac{\mathrm{d}L}{\mathrm{d}T}\right)\frac{n_0^3}{4}(1 + v)(p_{11} - p_{12});$$

v is the Poisson coefficient;

$$\tilde{T}(r) = \frac{1}{h}\int_0^h T(r, z)\mathrm{d}z$$

is the thickness-averaged disc temperature. One can see from expressions (7)–(10) that the expressions for δ_{lin} and Ψ for the [111] orientation can be derived from the corresponding expressions for the [001] orientation by the formal change

$$\xi \to 1, \quad Q_{\text{disc}} \to Q_{\text{disc}}(1 + 2\xi)/3. \tag{11}$$

All results given below pertain only to the [001] orientation, bearing in mind that the results for the [111] can be easily obtained with the change (11). We note that the reverse [111]-to-[001] orientation pass is impossible. For all elements made of any type of glass, $\xi = 1$. For $\xi = 1$, expressions (7)–(10) (and all results given below) for the [001] and [111] orientations coincide. In this case, $\Psi = \varphi$ and δ_{lin} is independent of either φ or θ.

Note that in expression (9) there appears the temperature gradient rather than the temperature itself. To determine the gradient requires integrating the heat conduction equation

$$\frac{\mathrm{d}^2T}{\mathrm{d}z^2} + \frac{1}{r}\frac{\mathrm{d}}{\mathrm{d}r}\left(r\frac{\mathrm{d}T}{\mathrm{d}r}\right) = -\frac{\alpha I_0}{k}\exp\left(-\frac{r^{2m}}{r_0^{2m}}\right) \tag{12}$$

subject to the boundary condition

$$T(r, 0) = T(r, h) = T_0.$$

Here, α and k are the absorption coefficient and the thermal conductivity, respectively. Considering that the heat is removed across the faces, the second term in the left-hand side of Eqn (12) can be taken to be negligible for any beam-disc radius ratio. Then, it is easy to obtain the requisite expression for $\mathrm{d}\tilde{T}/\mathrm{d}r$:

$$\frac{\mathrm{d}\tilde{T}(r)}{\mathrm{d}r} \equiv \frac{\mathrm{d}}{\mathrm{d}r}\frac{1}{h}\int_0^h T(r,z)\mathrm{d}z$$

$$= \frac{\alpha\pi r_0^2 I_0}{k}\frac{h^2}{6\pi r_0^2}\frac{m}{r}\frac{r^{2m}}{r_0^{2m}}\exp\left(-\frac{r^{2m}}{r_0^{2m}}\right). \quad (13)$$

Strictly speaking, the problem under consideration corresponds to the boundary conditions of the third kind, and therefore expression (13) should be regarded as an approximate solution which is in a rather good agreement with the exact solution and experimental results. This is borne out by the results obtained in the analysis of thermal processes in the active elements of solid-state lasers (see, for instance, Ref. [14]). We note that the second term in the left-hand side of Eqn (12) can no longer be neglected for large m. We substitute expression (13) expression (9) and the result in expressions (4)–(6) to obtain, upon integration of formula (2) in view of formula (3), the depolarisation ratio γ. For angles θ optimised for minimum depolarisation ratio [1], for each of the schemes we arrive at the formulas

$$\gamma_0^{\min} = \frac{1}{\pi^2}A_1(m)p^2\left(\frac{h}{r_0}\right)^4, \quad (14)$$

$$\gamma_{\mathrm{L}}^{\min} = \frac{8}{\pi^4}A_2(m)p^4\xi^2(2a^2+b^2)\left(\frac{h}{r_0}\right)^8, \quad (15)$$

$$\gamma_{\mathrm{R}}^{\min} = \frac{6}{\pi^4}A_2(m)a^2\left(1+\frac{2}{3}\xi^2+\xi^4\right)p^4\left(\frac{h}{r_0}\right)^8, \quad (16)$$

where

$$p = \frac{L}{\lambda}Q_{\mathrm{disc}}\frac{\alpha P_0}{k}$$

is a dimensionless quantity which characterises the transmitted radiation power P_0;

$$A_1 = \frac{m^2}{9}\int_0^\infty \exp(-t^m)$$

$$\times\frac{1}{t^2}\left[\int_0^t u^m\exp(-u^m)\mathrm{d}u\right]^2\mathrm{d}t\Big/\int_0^\infty\exp(-u^m)\mathrm{d}u, \quad (17)$$

$$A_2 = \frac{m^4}{3^4}\int_0^\infty \exp(-t^m)$$

$$\times\frac{1}{t^4}\left[\int_0^t u^m\exp(-u^m)\mathrm{d}u\right]^4\mathrm{d}t\Big/\int_0^\infty\exp(-u^m)\mathrm{d}u \quad (18)$$

are constants defined by the beam shape.

Thin disc ($h \ll r_0$, $r_0 \simeq R$). Under this approximation we can, as before, use the planar-stressed-state condition and hence formula (9). At the same time, the heat propagates radially and the second term in the left-hand side of Eqn (12) cannot be neglected.

For the solution of Eqn (12) it will be assumed that the side disc surface is thermally well insulated and the heat does not pass across it, and that temperature T_0 is maintained at the disc faces. Then, the boundary conditions for the heat conduction equation are of the form

$$\left.\frac{\mathrm{d}T(r,z)}{\mathrm{d}r}\right|_{r=R} = 0, \quad (19)$$

$$T(r,0) = T(r,h) = T_0. \quad (20)$$

We solve Eqn (12) by separating the variables to obtain

$$T(r,z) = T_0 + \frac{\alpha P_0}{\pi k r_0^2}\sum_{n,k=1}^{\infty} C_{nk}\sin\left(\frac{\pi n}{h}z\right)J_0\left(\frac{\mu_k}{R}r\right), \quad (21)$$

where

$$C_{nk} = \frac{2[1-(-1)^n]}{\pi n\left[(\mu_k/R)^2+(\pi n/h)^2\right]}$$

$$\times\int_0^{R^2/r_0^2}\exp(-u^m)J_0\left(\frac{\mu_k}{R}r_0\sqrt{u}\right)\mathrm{d}u\Big/\int_0^{R^2/r_0^2}J_0^2\left(\frac{\mu_k}{R}r_0\sqrt{u}\right)\mathrm{d}u;$$

J_i are the Bessel functions; μ_k satisfies the equation $J_1(\mu_k) = 0$.

By performing the requisite calculations, it is easy to obtain the minimal depolarisation ratio, which will be expressed by formulas (14)–(16). In this case, however, the quantities $A_{1,2}$ depend on the disc dimensions and the laser beam radius:

$$A_1 = \sum_{n,k=1}^{\infty}\left\{\frac{4[1-(-1)^n]}{\pi^2 n}\frac{C_{nk}}{h^2}\right\}^2\int_0^{R^2/r_0^2}\exp(-u^m)$$

$$\times\left[J_2\left(\frac{\mu_k}{R}r_0\sqrt{u}\right)\right]^2\mathrm{d}u\Big/\int_0^{R^2/r_0^2}\exp(-u^m)\mathrm{d}u, \quad (22)$$

$$A_2 = \sum_{n,k=1}^{\infty}\left\{\frac{4[1-(-1)^n]}{\pi^2 n}\frac{C_{nk}}{h^2}\right\}^4\int_0^{R^2/r_0^2}\exp(-u^m)$$

$$\times\left[J_2\left(\frac{\mu_k}{R}r_0\sqrt{u}\right)\right]^4\mathrm{d}u\Big/\int_0^{R^2/r_0^2}\exp(-u^m)\mathrm{d}u. \quad (23)$$

General case (R, $r_0 \simeq h$). When the beam radius is comparable with the disc thickness, the planar-stressed disc state approximation should be abandoned and use should be made of a more general expression for the linear birefringence. Taking advantage of the relations between the elastic deformation and mechanical stress tensors ε and σ for a cylinder of arbitrary form [13] and the procedure described in Ref. [10] it is possible to derive the following expression for δ_{lin}:

$$\delta_{\mathrm{lin}} = N\frac{2\pi}{\lambda}\left[\frac{1+\xi^2\tan^2(2\Psi-2\theta)}{1+\tan^2(2\Psi-2\theta)}\right]^{1/2}\frac{n_0^3}{2}(p_{11}-p_{12})$$

$$\times\int_0^h[\sigma_{rr}(r,z)-\sigma_{\varphi\varphi}(r,z)]\mathrm{d}z. \quad (24)$$

We employed the method considered in Ref. [15] to find the elements of the stress tensor. In this method, the displace-

ment vector is sought as the sum of the partial solution of inhomogeneous and the general solution of homogeneous Navier–Stokes equations. In this case, the temperature distribution in the disc is defined by formula (21). The integral depolarisation ratio in this case, too, can be brought to form (14)–(16), where $A_{1,2}$ are of the form

$$A_1 = \int_0^{R^2/r_0^2} \left[t_1(r_0\sqrt{u}) + t_2(r_0\sqrt{u})\right]^2 \times \exp(-u^m)\mathrm{d}u \Big/ \int_0^{R^2/r_0^2} \exp(-u^m)\mathrm{d}u, \quad (25)$$

$$A_2 = \int_0^{R^2/r_0^2} \left[t_1(r_0\sqrt{u}) + t_2(r_0\sqrt{u})\right]^4 \times \exp(-u^m)\mathrm{d}u \Big/ \int_0^{R^2/r_0^2} \exp(-u^m)\mathrm{d}u. \quad (26)$$

Here,

$$t_1(r) = 4\frac{1+v}{1-v}\int_0^\infty \left(\frac{k}{h}\right)^2 \mathrm{d}k\left[J_0(kr) - 2\frac{J_1(kr)}{kr}\right]\sum_{n,k=1}^{\infty} W_{nk};$$

$$t_2(r) = \frac{4}{1-2v}\int_0^\infty \left(\frac{k}{h}\right)^2 k\mathrm{d}k\left[J_0(kr) - 2\frac{J_1(kr)}{kr}\right]f(kh);$$

$$W_{nk} = \frac{[1-(-1)^n]C_{nk}}{\pi n}\frac{k^2h^2}{k^2h^2+\pi^2n^2}\frac{R^3J_0(\mu_k)J_1(kR)}{(kR)^2-\mu_k^2};$$

$$f(y) = \frac{2(1-2v)}{\sinh y + y}\frac{1+v}{1-v}\left[1+(1-2v)\frac{\sinh y}{y}\right]\int_0^\infty \rho\mathrm{d}\rho \times \int_0^h \mathrm{d}\eta J_0(k\rho)\frac{T(\rho,\eta)\sinh(kh/2)\cosh(k\eta - kh/2)}{k\sinh(kh)}.$$

3. Effect of the temperature dependence of the Verdet constant and Fresnel reflections

Let us estimate the significance of effects neglected in the derivation of formulas (14)–(16). It will be assumed that the variation of the Verdet constant V over the cross section is small in comparison with the constant itself. Then, the expression for the angular displacement of the plane of polarisation Φ for each Faraday element can be written in the following way:

$$\Phi(r) = \Phi_0\left\{1 + \left(\frac{1}{V}\frac{\mathrm{d}V}{\mathrm{d}T}\right)\left[\tilde{T}(r) - \tilde{T}(0)\right]\right\}. \quad (27)$$

The constant Φ_0 can be selected in such a way as to minimise the depolarisation ratio. Upon carrying out the calculation similarly to Ref. [3] it is easy to obtain the depolarisation ratio γ_V arising from the temperature dependence of the Verdet constant. For a Gaussian beam, the expression for this depolarisation ratio is of the form

$$\gamma_V = 3.6\times10^{-5}\left(\frac{\lambda}{LQ_{\mathrm{disc}}}\right)^2\left(\frac{1}{V}\frac{\mathrm{d}V}{\mathrm{d}T}\right)^2 p^2\left(\frac{h}{r_0}\right)^4. \quad (28)$$

We compare it with the depolarisation ratio arising from the photoelastic effect. For a TGG crystal we take $V^{-1}(\mathrm{d}V/\mathrm{d}T) = 3.5\times10^{-3}$ K^{-1} [16], $L/\lambda = 3\times10^4$, and $Q_{\mathrm{disc}} = 1.9\times10^{-6}$ K^{-1} [17] to obtain $\gamma_V/\gamma_0^{\min} = 1.4\times10^{-4}$. Therefore, the temperature dependence of the Verdet constant can be neglected in comparison with the photoelastic effect when the first scheme is used (Fig. 1a). A comparison of formula (28) with formulas (15) and (16) shows that the quantity γ_V is also insignificant when use is made of the second and third schemes (Figs 1b and 1c).

Let us estimate the effect of Fresnel reflections. The radiation which passes through the Faraday isolator reflects twice from the disc surfaces to form a wave propagating parallel to and in the same direction with the transmitted wave. The intensity of this wave is R_F^2 times lower (R_F is the intensity reflectivity) and the polarisation is rotated by an additional angle corresponding to the additional radiation pass through the magnetoactive medium. We neglect the beams arising upon four reflections and take into account that $R_F \ll 1$ to obtain the following expressions for the depolarisation ratio in the corresponding schemes:

$$\gamma_0^F = R_F^2\left[1 + \sum_{n=1}^{N} 4(N-n)\sin^2\left(\frac{n\pi}{2N}\right)\right] \approx \frac{3(N^2+1)}{5}R_F^2, \quad (29)$$

$$\gamma_L^F = R_F^2\left[2 + 16\sum_{n=1}^{N/2}\left(\frac{N}{2}-n\right)\sin^2\left(\frac{n\pi}{2N}\right) + 2 + 4\sum_{n=1}^{N/2}\left(\frac{N}{2}-n\right)\sin^2\left(\frac{n\pi}{2N}\right)\right], \quad (30)$$

$$\gamma_R^F = R_F^2\left[1 + 4\sum_{n=1}^{N}(N-n)\sin^2\left(\frac{n\pi}{2N}\right) + 2 + 4\sum_{n=1}^{N/2}\left(\frac{N}{2}-n\right)\sin^2\left(\frac{n\pi}{2N}\right)\right]. \quad (31)$$

The dependences of $\gamma_{0,L,R}^F$ on the number of discs are plotted in Fig. 2. It is noted that increasing the number of discs increases the quantities $\gamma_{0,L,R}^F$ and decreases $\gamma_{0,L,R}^{\min}$, i.e. to minimise the depolarisation ratio in each specific case requires selecting the optimal number of discs. At the same time, for $R_F < 0.2\,\%$ (which does not present technical difficulties) the values of $\gamma_{0,L,R}^F$ are rather small.

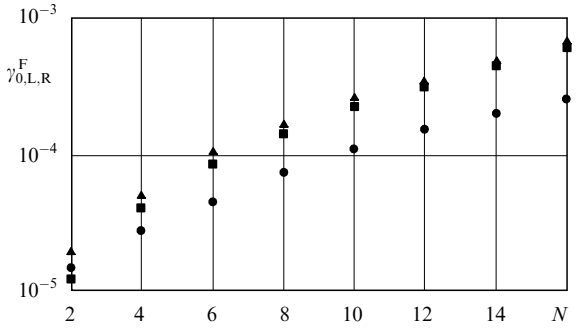

Figure 2. Depolarisation ratio arising from Fresnel reflections γ_0^F (■), γ_L^F (●) and γ_R^F (▲) as functions of the number of discs employed N for $R_F = 0.2\,\%$.

4. Disc cooling

The most significant drawback of the disc-like geometry is cooling via the optical surfaces, although this method of

cooling is used in practice [18]. We estimate the temperature gradients occurring in the disc.

Let us assume that the cooling is performed as shown in Fig. 1. We also assume the discs are square and the heat sources are uniformly distributed over the disc. To avoid turbulence-induced phase distortions, it is necessary to ensure laminarity of the cooling gas flow. We also assume the gas temperature to be uniformly distributed along the z axis; to this end, use should be made of a gas with a high thermal conductivity, for instance helium, whose thermal conductivity coefficient is equal to $0.152\ \mathrm{W\ K^{-1}\ m^{-1}}$. Ensuring laminarity of the helium flow necessitates fulfilment of the condition $Ul < 0.08\ \mathrm{m^2\ s^{-1}}$ [19], where U is the average gas velocity and $2l$ is the interdisc gap. In the stationary regime, along the optical disc surface there arises an additional temperature gradient [18]

$$\frac{\mathrm{d}T}{\mathrm{d}x} = \frac{\alpha h P_0}{4 U l c_\mathrm{g} R^2}, \tag{32}$$

where c_g is the heat capacity of the gas. We note that $\alpha h P_0$ is the power of heat release in one disc. Let $\alpha = 10^{-3}\ \mathrm{cm^{-1}}$, $Ul = 0.08\ \mathrm{m^2\ s^{-1}}$, $P_0 = 10\ \mathrm{kW}$, $h = 3$ mm, $c_\mathrm{g} = 555\ \mathrm{J\ K^{-1}\ m^{-3}}$, and $R = 1$ cm, then $\mathrm{d}T/\mathrm{d}x = 1.7\ \mathrm{K\ cm^{-1}}$. Therefore, at the disc faces there arises an additional temperature gradient along the x axis, which results in a redistribution of photoelastic stress and the occurrence of additional depolarisation. However, this effect may be cancelled out in the radiation pass through the next disk (which is winded in the opposite direction).

Cooling two disc faces with oppositely directed gas flows (see Fig. 1) leads to the emergence of a temperature gradient $\mathrm{d}T/\mathrm{d}z$ along the z axis. For the above parameters, $\mathrm{d}T/\mathrm{d}z = 11\ \mathrm{K\ cm^{-1}}$. These values of the temperature gradient may cause the disruption of a disc made of magnetoactive glass. To increases the transmitted radiation power, use should be made of firmer discs of TGG monocrystals or a polycrystalline TGG ceramics [12, 20]. Furthermore, the longitudinal gradients may be significantly weakened if all the discs are blown on from one side (for instance, in a downward direction), because the refrigerant temperatures at the right and left disk boundaries will be equal. The optimal cooling geometry invites further investigation.

5. Discussion and conclusions

The dimensionless parameter p is, by its physical significance, the normalised power of laser radiation. For the TGG crystals, the thermal conductivity coefficient is $k = 7.4\ \mathrm{W\ K^{-1}\ m^{-1}}$, and the ratio L/λ can be assumed to be equal to 30000 for our estimates. The absorption in TGG crystals differs several-fold for different samples, even though the samples may be grown in one firm [10, 11]. For TGG with a minimal [10] absorption ($\alpha Q_\mathrm{disc} = 2.5 \times 10^{-7}\ \mathrm{K^{-1}\ m^{-1}}$), the parameter $p = 1$ for a laser radiation power $P_0 = 1$ kW. At the same time, for magnetoactive glasses, the parameter $p \approx 1$ for $P_0 = 100$ W.

Figure 3 shows the dependences of depolarisation ratio on the parameter p for disc- and rod-like geometries of the magnetoactive elements of the Faraday isolator. Using discs with an aspect ratio $r_0/h = 2$ in the first scheme allows to reject rods even for $p > 2$. Therefore, there is no need to employ the second and third schemes. The advantage of

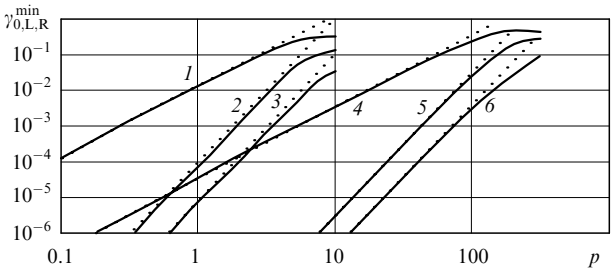

Figure 3. Depolarisation ratio of the Faraday isolator $\gamma_0^{\min}$ (*1*, *4*), $\gamma_\mathrm{L}^{\min}$ (*2*, *5*), and $\gamma_\mathrm{R}^{\min}$ (*3*, *6*) as functions of the parameter p for $\xi = 1$ for a rod-like (*1–3*) and disc-like geometries with an aspect ratio $r_0/h = 2$ (*4–6*). Solid curves represent the results of numerical calculations and the dotted lines the calculation under the approximation $\delta_\mathrm{lin} \ll 1$.

discoid Faraday isolators only increases with increase in aspect ratio. However, employing thin discs increases them in number. Employing discs in the second and third schemes makes it possible to make Faraday isolators operating at a power of tens of kilowatts.

Interestingly, when r_0 approaches R for large m, the depolarisation ratio decreases sharply (Fig. 4). This is due to equalisation of the temperature over the disc radius. However, applying this mechanism of depolarisation ratio suppression presents serious technical difficulties (super-Gaussian beams with a large index m are required, as is the coincidence of r_0 and R with an accuracy of better than 5 %).

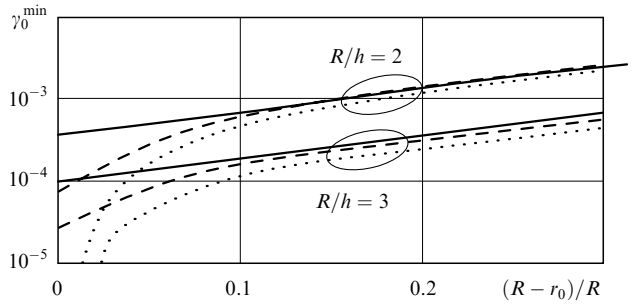

Figure 4. Depolarisation ratio of the Faraday isolator $\gamma_0^{\min}$ as functions of the disc parameters for $p = 6$ when use is made of a Gaussian (solid curves, $m = 1$), super-Gaussian (dashed lines, $m = 10$), and Π-shaped (dotted lines, $m = \infty$) beams.

A comparison of the depolarisation ratio magnitudes in the three cases considered in Section 2 shows that for $r_0 > 2h$ it is rather well described by the formulas of the first and second approximations (see Table 1), and calculations by cumbersome formulas (25) and (26) is unnecessary.

Table 1. Relative error of depolarisation ratio calculations under two approximations compared to exact calculations by formulas (25) and (26).

r_0/h	Approximation	
	$h \ll r_0 \ll R$	$h \ll r_0,\ r_0 \simeq R$
1.5	86 %	16 %
2	38 %	6 %
2.5	16 %	2.8 %
3	4 %	0.8 %

For a multikilowatt power, the linear birefringence may become significantly stronger and the condition $\delta_{\text{lin}} \ll 1$ will be violated. In this case, formulas (4)–(6) are incorrect and numerical calculations are required to determine the depolarisation ratio. The results of calculations for a Gaussian beam with an aspect ratio $r_0/h = 2$ are given in Fig. 3. One can see formulas (14)–(16) yield a rather accurate result up to $p = 100$. When the aspect ratio is equal to 1.5, the discrepancy between analytical and numerical calculations is observed even for $p > 40$. Therefore, formulas (14)–(16), which were derived under the assumption that $\delta_{\text{lin}} \ll 1$, are quite adequate in the multikilowatt power range.

We summarise the results of investigations performed for Faraday isolators with a disc-like geometry:

1. The depolarisation ratio arising from the temperature dependence of the Verdet constant is negligible in comparison with the depolarisation ratio due to photoelastic effect. The Fresnel reflections for a reflection coefficient $R_F < 0.2\,\%$ are also responsible for a significant depolarisation ratio.

2. The depolarisation ratio is scarcely affected by the boundary conditions at the side disc surface.

3. The disc-like geometry complicates heat removal. Even blowing on discs with helium gives rise to substantial temperature gradients, which may be responsible for the occurrence of additional depolarisation ratio. The optimal cooling geometry calls for further investigation.

4. The depolarisation ratio is proportional to the squared power and inversely proportional to the fourth power of the aspect ratio for the conventional scheme (Fig. 1a), and is proportional to the fourth power of the radiation power and inversely proportional to the eighth power of the aspect ratio for new schemes (Figs 1b and 1c).

5. By replacing rods with discs it is possible to obtain a depolarisation ratio of 30 dB for a power of 10 kW, provided the disc thickness is smaller than the radius of the Gaussian beam.

Acknowledgements. The authors thank A.K. Potemkin for helpful discussions and assistance.

References

1. Khazanov E.A. *Kvantovaya Elektron.*, **26**, 59 (1999) [*Quantum Electron.*, **29**, 59 (1999)].
2. Eichler H.J., Mehl O., Eichler J. *Proc. SPIE Int. Soc. Opt. Eng.*, **3613**, 166 (1999).
3. Khazanov E.A., Kulagin O.V., Yoshida S., Tanner D., Reitze D. *IEEE J. Quantum Electron.*, **35**, 1116 (1999).
4. Andreev N.F., Palashov O.V., Potemkin A.K., Raitsi D.Kh., Sergeev A.M., Khazanov E.A. *Kvantovaya Elektron.*, **30**, 1107 (2000) [*Quantum Electron.*, **30**, 1107 (2000)].
5. Khazanov E.A. *Kvantovaya Elektron.*, **30**, 147 (2000) [*Quantum Electron.*, **30**, 147 (2000)].
6. Khazanov E., Andreev N., Babin A., Kiselev A., Palashov O., Reitze D. *J. Opt. Soc. Am. B*, **17**, 99 (2000).
7. Khazanov E.A. *Kvantovaya Elektron.*, **31**, 351 (2001) [*Quantum Electron.*, **31**, 351 (2001)].
8. Andreev N.F., Katin E.V., Palashov O.V., Potemkin A.K., Raitsi D.Kh., Sergeev A.M., Khazanov E.A. *Kvantovaya Elektron.*, **32**, 91 (2002) [*Quantum Electron.*, **32**, 91 (2002)].
9. Khazanov E.A., Anastasiyev A.A., Andreev N.F., Voytovich A., Palashov O.V. *Appl. Opt.*, **41**, 2947 (2002).
10. Khazanov E., Andreev N., Palashov O., Poteomkin A., Sergeev A., Mehl O., Reitze D. *Appl. Opt.*, **41**, 483 (2002).
11. Mueller G., Amin R.S., Guagliardo D., McFeron D., Lundock R., Reitze D.H., Tanner D.B. *Classical and Quantum Gravity*, **19**, 1793 (2002).
12. Khazanov E. *Appl. Opt.*, **43**, 1907 (2004).
13. Landau L.D., Lifshits E.M. *Theory of Elasticity* (Oxford: Pergamon Press, 1986).
14. Mezenov A.V., Soms L.N., Stepanov A.I. *Termodinamika tverdotel'nykh lazerov* (Thermodynamics of Solid-State Lasers) (Leningrad: Mashinostroenie, 1986).
15. Olmstead M.A., Amer N.M., Kohn S. *Appl. Phys. A*, **32**, 141 (1983).
16. Barnes N.P., Petway L.P. *J. Opt. Soc. Am. B*, **9**, 1912 (1992).
17. Khazanov E., Andreev N., Mal'shakov A., Palashov O., Poteomkin A., Sergeev A., Shaykin A., Zelenogorsky V., Ivanov I., Amin R., Mueller G., Tanner D.B., Reitze D.H. *IEEE J. Quantum Electron.*, **40** (10) (2004).
18. Eimerl D. *IEEE J. Quantum Elecron.*, **23**, 575 (1987).
19. Petukhov B.S. *Teploobmen i soprotivlenie pri laminarnom techenii zhidkosti v trubakh* (Heat Exchange and Resistance in the Laminar Fluid Flow in Pipes) (Moscow: Energiya, 1967).
20. Kagan M.A., Khazanov E.A. *Appl. Opt.*, **43** (32) (2004).